Three-State Conical Intersections in Nucleic Acid Bases

Spiridoula Matsika*

Department of Chemistry, Temple University, Philadelphia, PA, 19122

Received: March 15, 2005; In Final Form: June 2, 2005

The involvement of three-state conical intersections in the photophysics and radiationless decay processes of the nucleobases has been investigated using multireference configuration interaction methods. Three-state conical intersections have been located for the pyrimidine base, uracil, and the purine base, adenine. In uracil, a three-state degeneracy between the S_0, S_1, and S_2 states has been located at 6.2 eV above the ground-state minimum energy. This energy is 0.4 eV higher than vertical excitation to S_2 and at least 1.3 eV higher than the two-state conical intersections found previously. In adenine, two different three-state degeneracies between the S_1, S_2, and S_3 states have been located at energies close to the vertical excitation energies. The energetics of these three-state conical intersections suggest they can play a role in a radiationless decay pathway present in adenine. The existence of two different seams of three-state conical intersections indicates that these features are common and complicate the potential energy surfaces of adenine and possibly many other aromatic molecules.

1. Introduction

Although the importance of two-state conical intersections in nonadiabatic processes has been established,[1,2] the occurrence and relevance of accidental three-state conical intersections is only now emerging. Three-state degeneracies imposed by symmetry had been studied in the context of the Jahn−Teller problem for many decades,[3] but only minor attention had been given to accidental three-state degeneracies in molecules.[4] Because most molecular systems in nature have low or no symmetry, these accidental intersections may have a great impact on the photophysics and photochemistry of molecular systems, as has been found in accidental two-state intersections.[1,2,5,6] Three-state degeneracies can provide a more efficient relaxation pathway when more than one interstate transition is needed, they introduce more complicated geometric phase effects,[7−9] and they can affect the dynamics and available pathways.[10] The exact way these features affect the dynamical behavior of molecules is a question that has yet to be studied extensively. According to the noncrossing rule,[11] three states can become degenerate in a subspace of dimension $N^{\text{int}} - 5$, where N^{int} is the number of internal coordinates. For this reason, they cannot be found in molecular systems with less than five internal coordinates. Even in systems with enough degrees of freedom, the dimensionality makes their location difficult. Until recently, the perception was that three-state degeneracies are extremely rare, mostly because of the inability to locate them. Recent developments of efficient algorithms, however, have made these calculations possible and have revealed that three-state conical intersections exist in many organic radicals[12−14] and may play an important role on their spectroscopic or photophysical properties. Both excited-state dynamics and ground-state vibrational spectra can be affected by these features. More recent studies indicate the existence of three-state conical intersections in closed-shell systems also.[10,15]

Systems with high density of electronic states are more likely to exhibit three-state crossings if they have enough degrees of freedom. Examples of systems with many, closely spaced, excited electronic states are radicals with closely spaced Rydberg excited states, such as the ethyl and allyl radical, where the 3s and 3p Rydberg states can intersect.[12,13] Another very important category of molecules that have many electronic states close in energy are conjugated systems. An example of a conjugated open-shell system is the pyrazolyl radical, which has been found to have three-state conical intersections only 3000 cm^{-1} above the ground-state minimum.[14] In this case, the ground state is one of the degenerate states, and complicated vibronic spectra are expected, and have been observed experimentally.[16]

In a closed shell aromatic system, excitations to π^* orbitals create a manifold of excited states. Some of the most important molecules in nature, such as the nucleobases discussed here, are closed-shell aromatic molecules. The excited-state dynamics of nucleic acid bases has gained much attention recently.[17] The problem is important because of the biological significance of the bases. These bases are the dominant chromophores in nucleic acids, and their photochemical and photophysical properties are implicated in the behavior of the nucleic acids upon irradiation.[18−20] The excited-state lifetimes have been reported recently using many different techniques.[21−39] These studies report lifetimes on the order of femtoseconds and suggest that nonradiative relaxation proceeds on an ultrafast time scale to the ground state, with the extra energy being transformed into heat.

The involvement of two-state conical intersections in the nucleobases has been examined by several groups. Conical intersections were found in cytosine,[40,41] uracil,[42] and adenine,[43,44] and pathways were suggested that could explain mechanisms for radiationless decay to the ground state. A recent work examined three-state near degeneracies in cytosine.[15] A near-degeneracy point was found ca. 1.5 eV higher than the vertical excitation to the bright state of cytosine using perturbative methods (CASPT2). At the complete-active space self-consistent-field (CASSCF) level this point is ca. 2 eV lower and close to vertical excitations. These discrepancies in the energetics are probably due to the fact that an algorithm to locate

* Corresponding author. E-mail address: smatsika@temple.edu.

10.1021/jp0513622 CCC: $30.25
Published on Web 07/29/2005

three-state conical intersections was not used, so these points are not optimized points on the seam. Although the authors propose that the three-state intersection is important in the radiationless decay, the energetics at the CASPT2 level suggest the opposite.

The purpose of this work is to examine the different possibilities in which three-state conical intersections may appear in the potential energy surfaces of the nucleobases and to investigate in which cases they are expected to be important. Three-state conical intersections in two nucleobases, uracil and adenine, are reported using multireference configuration interaction (MRCI) methods. Section 2 discusses the theoretical methods used for obtaining the electronic energies and gradients and locating conical intersections. Three-state conical intersections have been located between the S_0, S_1, and S_2 states in uracil and between the S_1, S_2, and S_3 states in adenine. The most stable tautomer of adenine, 9H-adenine, is examined. These intersections are presented and discussed in Section 3, and conclusions are given in Section 4.

2. Methods

The adiabatic energies and wave functions were determined at the MRCI level using orbitals from a state-averaged CASSCF procedure. The double-ζ plus polarization (cc-pvdz) Gaussian basis sets of Dunning were used for all atoms.[45] Optimizations were carried out using first-order MRCI expansions. Single-point MRCI calculations, with expansions, including single and double excitations, were used to refine the energies. The algorithm for locating three-state conical intersections has been described previously.[12] A modified version of the COLUMBUS suite of programs[46] was used, where the algorithms for locating two- and three-state conical intersections[12,47,48] have been included. The algorithms use analytic gradients for MRCI wave functions available in COLUMBUS.[49] The specific details of the multireference calculations for uracil and adenine are given below.

2.1. Uracil. The justification and details of the choice of the MRCI expansions used in uracil are given in our previous work.[42] Here, a summary of these methods is provided. A state-averaged CASSCF was used, where the ground state and two excited singlet electronic states were included in the average. An active space with 12 electrons in 9 orbitals, denoted (12, 9), was used in both CASSCF and MRCI in the optimization calculations. The designation (n, m) is used here for an active space of n electrons in m orbitals. It was found previously that this active space, where the nine active orbitals were the eight π and one of the two n_O valence orbitals, gave energies very similar to the ones obtained from an active space that included all valence orbitals, eight π and both n_O orbitals. Two different MRCI expansions were used for the optimizations. In the first expansion, all σ electrons were frozen, and single excitations only were allowed out of the active space. The number of configuration state functions (CSFs) was 607 320, and this expansion is denoted here as MRCI1. In the second expansion, only the core 1s electrons were frozen, and single excitations were allowed out of the σ orbitals as well. This expansion consisted of 9 518 670 CSFs and is denoted MRCI1σ. MRCI1σ was used to reoptimize the three-state conical intersection because the inclusion of dynamical correlation changed the energies of degenerate states so that they became separated by more than 0.4 eV. This observation will be discussed further in Section 3. The energies were refined using an MRCI expansion with a (14, 10) reference space, which included $\sigma\pi$ correlation (denoted MRCI$\sigma\pi$) as described in the previous work.[42] This MRCI$\sigma\pi$ expansion consisted of ca. 100 million CSFs.

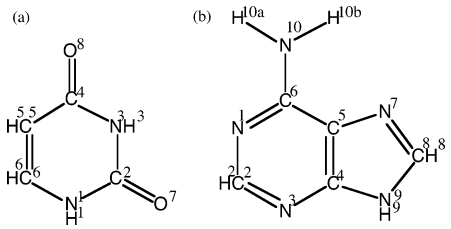

Figure 1. Molecular structure and atom numbering for (a) uracil and (b) adenine.

2.2. Adenine. Adenine has 10 π and 3 lone-pair n_N orbitals from the nitrogen atoms, giving 13 active orbitals with 18 electrons. An active space (18, 13) generates too many references in either the MCSCF or the MRCI procedures. However, the orbitals localized mainly on the five-membered ring do not participate in the first few excited states that we are interested in; rather it is the orbitals localized on the six-membered ring that are important for these states. Initial trials showed that a (12, 9) active space, where the nine orbitals were seven π and two n_N orbitals, was adequate for the lowest excited states. The orbitals were obtained from a state-averaged CASSCF using the (12, 9) active space and averaging over five singlet electronic states. MRCI expansions with references generated from this active space were used for all gradient calculations. As in uracil, two different expansions were generated. In the first one (denoted MRCI1), all σ electrons were frozen, and single excitations from the (12, 9) active space generated 770 616 CSFs. In the second (denoted MRCI1σ), only the 1s core electrons were frozen, and single excitations from the σ orbitals were allowed as well, giving 15 096 312 CSFs. MRCI1σ was used in adenine for the same reason it was used in uracil, to reoptimize a conical intersection when correlation changed the energy separation of the states by more than 0.4 eV.

Refinement of the energetics was obtained by using extended MRCI expansions. All single and double excitations from the (12, 9) active space and only single excitations from all σ orbitals were included. The 10 1s core orbitals and the 10 highest in energy virtual orbitals were kept frozen. The resulting expansion is denoted MRCI$\sigma\pi$ and includes ca. 200 million CSFs. In C_s symmetry, the resulting expansions for A' and A'' symmetries are 100 880 026 and 101 068 778 CSFs, respectively. When the geometry is almost coplanar, C_s symmetry is employed for single-point energy calculations using MRCI$\sigma\pi$ because the computational cost is significantly reduced.

3. Results and Discussion

The structure and conventional labeling of the atoms for uracil and adenine (9H-adenine) are shown in Figure 1. Below, we discuss the three-state conical intersections found in these molecules. The designation of conical intersections between two states, S_I, S_J, is *ciIJ* and between three states, S_I, S_J, S_K, is *ciIJK*. Geometries at a conical intersection *ciIJ* are given as $\boldsymbol{R}_x(ciIJ)$, and geometries of minimum energy points on a surface S_I as $\boldsymbol{R}_e(S_I)$.

3.1. Uracil. In a previous work, we located conical intersections in uracil between the S_2 and S_1 surfaces and between the S_1 and the ground state, S_0.[42] The two-state conical intersections in uracil facilitate efficient radiationless decay from the bright S_2 state to the ground state. Because a radiationless decay involves the three surfaces S_0, S_1, and S_2, the existence of a three-state conical intersection between these states could expedite the overall process if the seam is energetically accessible. Here, a three-state conical intersection between the three states participating in this mechanism has been located.

TABLE 1: Energies in eV for the Three Lowest States of Uracil at the Equilibrium of the Ground State $R_e(S_0)$ (vertical excitations) and at Conical Intersections $R_x(ciIJ)$ or $R_x(ciIJK)$[a]

	$R_e(S_0)$[b]	$R_x(ci12)$[b]	$R_x(ci01)$[b]	$R_x(ci012)$	$R_{x2}(ci012)$
S_0	**0**	2.15 (1.87)	**4.47** (3.96)	**6.83** (5.90)	(6.04)
S_1	5.44 (4.80)*	**5.37** (4.83)*	**4.47** (4.29)	**6.83** (6.37)*	(6.20)*
S_2	6.24 (5.79)	**5.37** (4.97)	7.62*	**6.83** (6.56)	(6.25)

[a] The energies in bold in each column correspond to the optimized degenerate states *I, J* or *I, J, K*. MRCI1 results are shown (the zero is set to −412.624433 au), and in parentheses are the single-point energies obtained using MRCI$\sigma\pi$ (the zero is set to −412.815540 au). States that have $n\pi^*$ character are designated with an * as superscript. [b] Taken from ref 42.

Table 1 gives the energy for the three-state conical intersection *ci*012, as well as the previous results of vertical excitation energies and two-state conical intersections. At the MRCI1 level, the minimum energy point on the seam, $\boldsymbol{R}_x(ci012)$, is 6.83 eV above the ground-state minimum. This energy is 0.6 eV higher than that of the vertical excitation to the bright state S_2 and 1.5 and 2.4 eV higher than that of the two-state conical intersections *ci*12 and *ci*01, respectively (at the MRCI1 level). The results for two-state conical intersections are taken from our previous work.[42]

When MRCI$\sigma\pi$ is used to recalculate the energies of S_0, S_1, and S_2 at the conical intersection $\boldsymbol{R}_x(ci012)$, they are found to be separated by 0.7 eV. This is because dynamical correlation affects the energy of the three states to different degrees. To improve the energy separation at the more correlated level, the three-state conical intersection is located using the MRCI1σ expansion, which includes single excitations from the σ orbitals. At this new geometry, which is denoted $\boldsymbol{R}_{x2}(ci012)$, the energies of the three states at the MRCI$\sigma\pi$ level are separated by 0.2 eV, and the average energy is 6.16 eV. The vertical excitation energy to the bright S_2 state is 5.8 eV using MRCI$\sigma\pi$, so the three-state degeneracy is 0.4 eV higher. The energy of the two-state conical intersections are again 1.3 and 2 eV lower than that of the three-state degeneracy. In summary, the *ci*012 conical intersection is energetically too high at every level of theory investigated, and this makes it less likely to directly participate in a radiationless decay mechanism.

The geometry at *ci*012 is shown in Figure 2 in comparison with the geometries at the minimum of the ground state and at the other two-state conical intersections, *ci*01 and *ci*12, from our previous work. A more complete list of internal coordinates is given as Supporting Information. The geometry at *ci*012 resembles the geometry at *ci*01, but the molecule is even further distorted. The most important distortion involves the oxygen O^8 atom. The C^4-O^8 bond distance increases by more than 0.1 Å, and O^8 is moved away from planarity. The dihedral angle $\angle O^8C^4N^3H^3$, which indicates the displacement of O^8 away from planarity, is between 0 and 6° in all other geometries, but increases to 39° at *ci*012. H^5 is still almost perpendicular to the original plane of the ring, as shown in Figure 2. The dihedral angle $\angle H^6C^6C^5H^5$ is 108° for the structures of both *ci*01 and *ci*012 conical intersections. $\boldsymbol{R}_{x2}(ci012)$ differs from $\boldsymbol{R}_x(ci012)$ mainly in the bond distances, which are shown in parentheses in Figure 2, but the main characteristics and dihedral distortions of the structures are similar.

The three-state conical intersection occurs when the two different seams *ci*01 and *ci*12 cross. When the C^5-C^6 bond stretches from 1.35 to 1.48 Å, the S_2 state ($\pi\pi^*$) is stabilized, while the S_1 ($n_O\pi^*$) is not affected, and the two states become degenerate, forming *ci*12. Breaking of the planarity of the ring

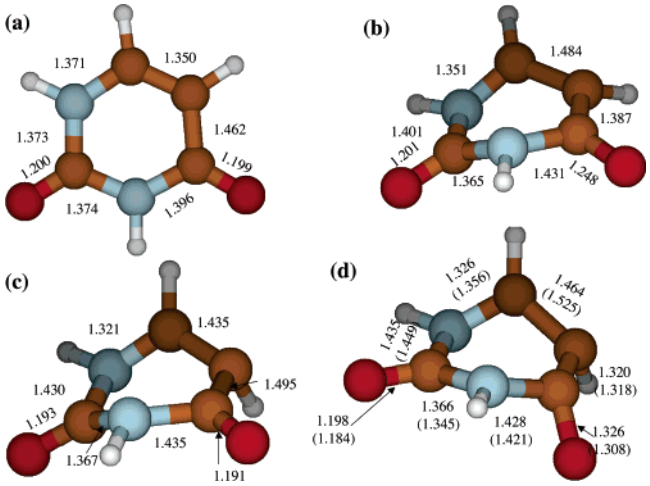

Figure 2. Geometry of uracil at (a) the S_0 minimum, (b) the S_1-S_2 conical intersection, (c) the S_0-S_1 conical intersection, and (d) the three-state $S_0-S_1-S_2$ conical intersection. All bond distances between non-hydrogen atoms are shown in Å. MRCI1 results are shown, except in (d), where the MRCIσ results are also shown in parentheses. More internal coordinates are given as Supporting Information.

by twisting of the C^5-C^6 bond and pyramidalization of C^5 destabilizes the ground state by more than 4 eV, causing it to meet the $\pi\pi^*$ state, forming the *ci*01 conical intersection. This distortion greatly destabilizes the $n_O\pi^*$ state which is 3 eV higher at the *ci*01 point. To bring together all three states, the geometry has to change in a way that the $n_O\pi^*$ state will be stabilized and the seam of *ci*01 will rise in energy to meet the $n_O\pi^*$. This happens when the C^4-O^8 bond is extended, while the nonplanar distortions remain.

3.2. Adenine. Adenine, like the other nucleobases, has ultrafast excited-state lifetimes and is expected to decay non-radiatively to the ground state, possibly through conical intersections of an excited state with the ground state. Indeed, theoretical work has shown the existence of conical intersections of $\pi\pi^*$, $n\pi^*$, or $\pi\sigma^*$ states with the ground state, and radiationless decay has been proposed through these conical intersections.[43,44] Here, we only focus on the excited states and the conical intersections between them. As will be seen in detail in the following section, the excited-states manifold for adenine is more complicated than that for uracil, and careful consideration of the interaction of excited states is important in order to understand its photodynamics. The closely spaced excited states suggest the existence of three-state conical intersections, and investigating this possibility is the main object of this work. Because adenine has not been studied previously using MRCI methods, before presenting the three-state conical intersections, the vertical excitation energies are presented and discussed. This is the starting point to determine which states are relevant and should be considered further.

3.2.1 Vertical Excitations. To calculate vertical excitation energies, the equilibrium geometry of adenine in the ground state is obtained by optimization at the MRCI1 level. The molecule is almost planar, but the amino group is pyramidalized ($\angle H^{10a}N^{10}C^6N^1 = 15°$, $\angle H^{10b}N^{10}C^6C^5 = -14°$), as was found in previous theoretical studies.[44,50−55] The geometry is shown in Figure 3 and is in good agreement with previous theoretical results. This figure includes only bond lengths, but a more complete list of internal coordinates is given as Supporting Information. Although the symmetry at equilibrium is deviated from C_s, it is computationally very advantageous to be able to employ symmetry in the calculations. For this reason, the effect of the nonplanar distortion on the vertical excitation energies

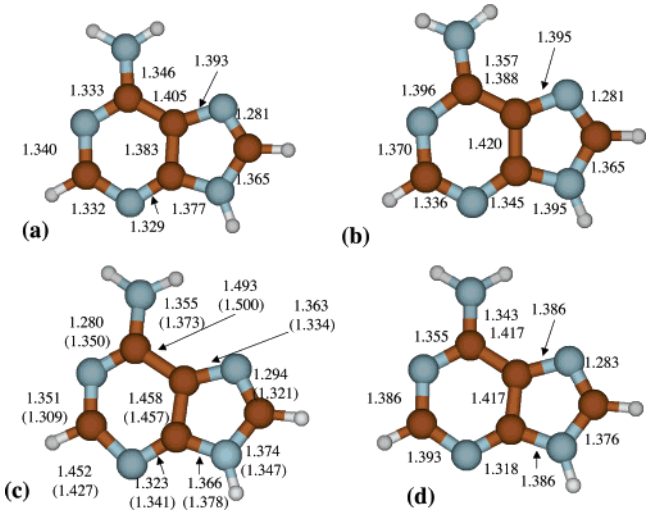

Figure 3. Geometry of adenine at (a) the S_0 minimum, (b) the three-state $S_1-S_2-S_3$ ($\pi\pi^*$, $n\pi^*$, $n\pi^*$) conical intersection, (c) the three-state $S_1-S_2-S_3$ ($\pi\pi^*$,$\pi\pi^*$, $n\pi^*$) conical intersection, and (d) the S_1-S_2 conical intersection. All bond distances between non-hydrogen atoms are shown in Å. MRCI1 results are shown, except in (c), where the MRCIσ results are also shown in parentheses. More internal coordinates are given as Supporting Information.

TABLE 2: Energies in eV for the Five Lowest States of Adenine at the Equilibrium Geometry of the Ground State $R_e(S_0)$ (vertical excitations) and at Conical Intersections $R_x(ciIJ)$ or $R_x(ciIJK)$[a]

	$R_e(S_0)$	$R_x(ci123)$	$R_x(ci123')$	$R_{x2}(ci123')$	$R_x(ci12)$
S_0	**0**	0.43 (0.28)	0.85 (0.75)	(0.73)	0.27 (0.20)
S_1	5.68 (5.67)	**5.72** (5.48)*	**6.24** (5.78)	(5.86)	**5.52** (5.24)*
S_2	5.85 (5.68)*	**5.72** (5.62)	**6.24** (5.84)*	(6.06)*	**5.52** (5.41)
S_3	6.55 (6.11)	**5.72** (5.67)*	**6.24** (6.18)	(6.06)	6.44 (6.07)
S_4	6.30 (6.25)*	6.91 (6.33)	7.72 (7.42)*	(7.37)*	6.31 (6.17)*

[a] The energies in bold in each column correspond to the optimized degenerate states *I*, *J* or *I*, *J*, *K*. MRCI1 results are shown (the zero is set to −464.68301 au), and in parentheses are the single-point energies obtained using MRCI$\sigma\pi$ (the zero is set to −464.923845 au). States that have $n\pi^*$ character are designated with an * as superscript.

has been investigated. The vertical excitation energies were calculated first using no symmetry and then using C_s symmetry. It was found that the effect is small, in the range 0.01−0.05 eV, allowing C_s symmetry to be used with the high-level, computationally expensive calculations.

Vertical excitation energies for adenine are given in Table 2. In this table, the common designation of excited states as S_1, S_2, etc., given by their energetic ordering, has been used. The character of the states is specified by using an * for the $n\pi^*$ (A'') states. At different points of the configurational space, this ordering changes. The energies at the MRCI1 and MRCI$\sigma\pi$ levels are listed. The excitation energies and even the ordering of the states are affected by the inclusion of dynamical correlation. The first two excited states are $n\pi^*$ and $\pi\pi^*$, and they are practically degenerate at the MRCI$\sigma\pi$ level, with the $\pi\pi^*$ slightly lower. The most dramatic effect of dynamical correlation is on the third excited-state S_3, which is a second $\pi\pi^*$ state. This state is at 6.55 eV at the MRCI1 level and at 6.11 eV using MRCI$\sigma\pi$, and consequently, the energy separation between the two $\pi\pi^*$ states changes from 0.9 to 0.4 eV as the theory improves. The fourth excited state is a second $n\pi^*$ state at 6.25 eV above the ground state at the MRCI$\sigma\pi$ level. In summary, there are four excited states, two $\pi\pi^*$ and two $n\pi^*$ states, at excitation energies between 5.5 and 6.3 eV. The ordering predicted at the MRCI$\sigma\pi$ level is $\pi\pi^*$, $n\pi^*$, $\pi\pi^*$, $n\pi^*$.

The excited states of adenine have been examined theoretically before using various methods, such as perturbation theory,[44,54,56] TDDFT,[43,52] and CIS.[55] Vertical excitations using TDDFT[52] gave energies 4.97, 5.08, and 5.35 eV for $n\pi^*$, $\pi\pi^*$, and $\pi\pi^*$ states, respectively. Earlier, CASPT2[56] vertical excitation energies were calculated to be 5.13, 5.20, 6.15, and 6.86 eV, while in a very recent work,[44] CASPT2 calculations give 4.85, 4.90, 5.50, and 5.68 eV. The ordering of the states in both cases is $\pi\pi^*$, $\pi\pi^*$, $n\pi^*$, $n\pi^*$. All calculations agree that the four lowest states are two $n\pi^*$ and two $\pi\pi^*$ states, but their relative ordering varies between different theoretical methods. In all cases, the two $\pi\pi^*$ states are close in energy. The $n\pi^*$ state, however, is predicted very close to the first $\pi\pi^*$ state by TDDFT and our MRCI results, but much higher than the $\pi\pi^*$ states when CASPT2 is used. It is obvious that the excitation energies and ordering of the states are very sensitive to the level of theory and correlation, and accurate benchmarks are not available for a definite comparison. MRCI methods are superior to TDDFT and CASPT2 when all electrons are correlated and the size of basis set is adequate. Here, it is not possible to fulfill both of these requirements, and so the best possible description must be compromised.

Experimental adiabatic energies have been obtained in the gas phase. Recent resonant two-photon ionization experiments[37] predict structured vibronic spectra where the $n\pi^*$ is the lowest excited state adiabatically at ca. 4.4 eV, but the $\pi\pi^*$ state is only 600 cm^{-1} higher at 4.47 eV. Nir et al.[30] and Lührs et al.[32] report a 0−0 band at 4.47 eV. This ordering, however, corresponds to adiabatic energies and cannot be compared directly with the vertical excitations because the ordering may change. The UV−vis absorption spectrum of adenine has a low-energy band with a peak around 4.9 eV in the gas phase and at 4.8 eV in aqueous solution.[57] The vertical excitation energies obtained in this work are higher than both the other theoretical results and the experimental absorption maximum, although in complicated spectra, like here, it is not always true that the absorption maximum corresponds to the vertical excitation.

Regardless of the above uncertainties, the results presented here, namely the presence and location of three-state conical intersections between the excited states, will not be affected qualitatively by changes in these energies. This claim is based on two facts. First, conical intersections were optimized using different MRCI expansions, and the additional correlation did not remove the degeneracies, but rather displaced them moderately. Second, the three-state conical intersections found exist independently of the ordering of states at vertical excitations.

3.2.2. $\pi\pi^* - n\pi^* - n\pi^*$ Conical Intersection. Starting at the equilibrium geometry, where the first three excited states have character $\pi\pi^*$, $n\pi^*$, $n\pi^*$ at the MRCI1 level, a conical intersection between these states was located. This conical intersection will be denoted *ci*123 and has energy 5.72 eV above the ground-state minimum at the MRCI1 level. At this level, the vertical excitation energies are 5.66, 5.85, and 6.27 eV, so the three-state conical intersection has about the same energy as vertical excitation to S_1. The fourth excited state ($\pi\pi^*$) is ca. 1 eV above the three-state conical intersection. Using MRCI$\sigma\pi$, the three energies are separated by less than 0.2 eV and have an average of 5.59 eV. This energy is lower than the vertical excitation energy to S_1 at the MRCI$\sigma\pi$ level, which is 5.67 eV. It is important to note that the intersecting states correlate to the S_1, S_2, S_4 states at vertical excitation but have become the S_1, S_2, S_3 states at this geometry, with the fourth state being at 6.33 eV. An S_3-S_4 conical intersection is probably the cause of this switching of states.

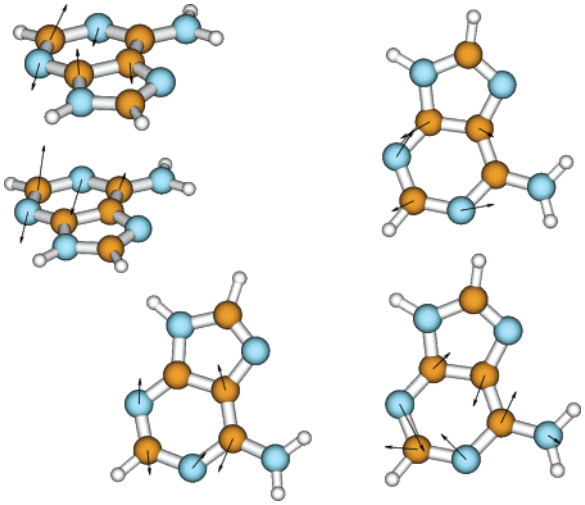

Figure 4. Five vectors defining the branching space for the *ci*123 conical intersection in adenine. The three top vectors correspond to the coupling vectors and the two bottom to the energy difference gradient vectors.

The geometry at *ci*123 is almost planar and is shown in Figure 3. Conical intersections involving the ground state, as the one found in uracil, require substantial geometrical distortions because, initially, the energy difference between the ground state and the excited state is more than 4 eV. Conical intersections, however, involving only excited states that are close energetically even at vertical excitation, require much smaller distortions. The distortions at *ci*123 involve mainly the bond distances in the six-membered ring because the states involved are described by orbitals mainly localized in this ring. The largest bond length distortions occur on C^6-N^1, which increases from 1.33 to 1.40 Å and on C^4-C^5, which increases from 1.38 to 1.42 Å. Excitation from the lone pair *n* to a π^* orbital weakens the C^6-N^1 double bond, and the distortions observed facilitate stabilization of the second $n\pi^*$ state so that it lowers its energy to meet S_1 and S_2.

The branching space for this three-state conical intersection is spanned by five vectors, instead of the usual two vectors in a two-state conical intersection.[6,58] Nuclear motion along these five vectors will remove the degeneracy of the states linearly. At the point of degeneracy, the vectors are not unique because the degenerate eigenfunctions can mix in any way. For two vectors, one can define an orthogonal transformation of the eigenfunctions to obtain the orthogonal unique vectors,[6] but this is not possible for the five vectors. In Figure 4, the five vectors are shown taken from a point slightly away from the degeneracy, so that the mixing of eigenvectors can be avoided. The visualization program MOLDEN[59] was used to generate the pictures of the vectors. The vectors involve mainly distortions of the six-membered ring, either in-plane bond distortions and bending, or out-of-plane ring-puckering motion. Because the symmetry is almost C_s, and the states crossing are $A'(\pi\pi^*)$, $A''(n\pi^*)$, and $A''(n\pi^*)$, the five vectors have symmetries $3a' + 2a''$. There are two vectors defined by the energy difference gradients of two pairs of states, and these are always totally symmetric (a'). The other three vectors correspond to the three couplings between the states, giving two a'' couplings and one a'. The a'' couplings correspond to coupling between each of the $n\pi^*$ states with the $\pi\pi^*$ state.

3.2.3. $n\pi^* - \pi\pi^* - \pi\pi^*$ Conical Intersection. A second seam of three-state conical intersections between the S_1, S_2, and S_3 states has been located in which the character of the states is $n\pi^*$, $\pi\pi^*$, $\pi\pi^*$. This conical intersection is denoted *ci*123′,

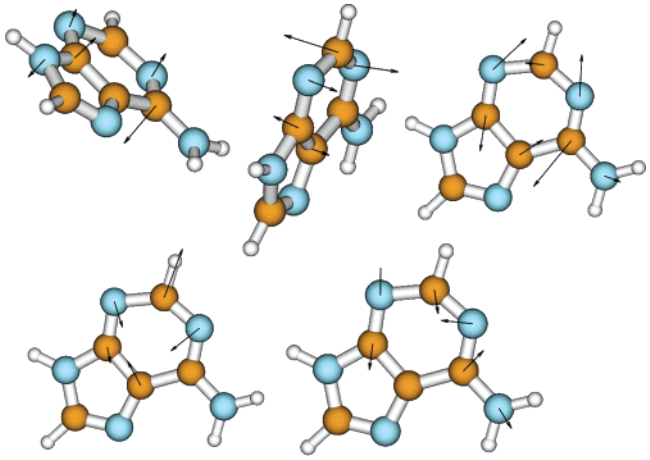

Figure 5. Five vectors defining the branching space for the *ci*123′ conical intersection in adenine. The three top vectors correspond to the coupling vectors and the two bottom to the energy difference gradient vectors.

and the energies are given in Table 2. The energy of the conical intersection is 6.24 eV at MRCI1, which is higher than *ci*123 but still in the range of vertical excitation energies. The fourth excited state, which is an $n\pi^*$ state, is more than 1.5 eV higher in energy. At the MRCI$\sigma\pi$ level, the energies are separated by 0.4 eV, with an average of 5.93 eV. To reduce the separation, this conical intersection was reoptimized using the MRCI1σ expansion in a similar way to that in uracil. At this new geometry, $\boldsymbol{R}_{x2}$(*ci*123′), the energies are separated by 0.2 eV with an average of 5.99 eV.

The geometry at the *ci*123′ conical intersection is shown in Figure 3. Like *ci*123, the structure is planar, but the *ci*123′ crossing involves larger distortions than those of the *ci*123 crossing, with the main changes involving bond distances in the six-membered ring. At this geometry, the $\pi\pi^*$ states come closer in energy, and the second $n\pi^*$ state is destabilized. The distortions that occur facilitate stabilization of the second $\pi\pi^*$ state and destabilization of the first $\pi\pi^*$ and the $n\pi^*$ states. The C^2-N^3, C^4-C,[5] and C^5-C^6 bond lengths increase by 0.12, 0.08, and 0.09 Å, respectively, in agreement with the fact that a $\pi\pi^*$ state is stabilized by relaxing the double bonds. The angles $C^4-N^3-C^2$ and the angles of N^{10} with the ring also change.

In Figure 5, the five vectors spanning the branching space are shown. Here, again, the symmetries of the vectors are $3a' + 2a''$, as can be seen in the figure. The vectors involve mainly distortions of the six-membered ring as was seen in *ci*123, although here, the N^9 atom is involved in one of the out-of-plane modes.

3.2.4. S_1-S_2 Conical Intersection Seam. Each of the three-state conical intersection seams has dimension $N^{\text{int}} - 5 = 39 - 5 = 34$. In the other five degrees of freedom, the degeneracy is lifted linearly. In three-dimensional subspaces of this five-dimensional branching space, the degeneracy can be lifted partially, and two of the three states will remain degenerate.[7,8,13] These two-state conical intersection seams originating from the three-state conical intersection have been studied in the allyl radical.[13] In adenine, different seams of two-state conical intersections originate from each of the three-state conical intersections, leading to a great number of two-state conical intersections at energies lower than the three-state seams. This picture will produce very complicated excited-state potential energy surfaces, and the photodynamics in these surfaces is expected to be affected.

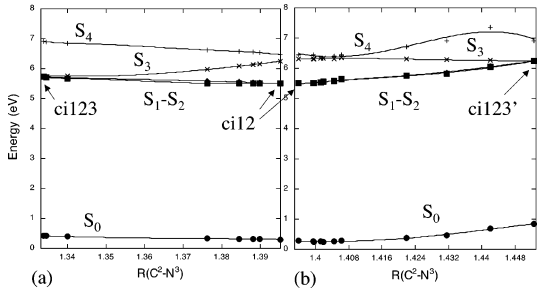

Figure 6. Minimum energy pathway (a) from the *ci*123 conical intersection to *ci*12 and (b) from the *ci*123′ conical intersection to *ci*12

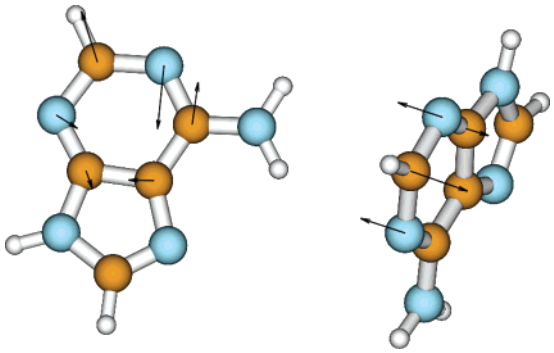

Figure 7. Two vectors defining the branching plane for the *ci*12 conical intersection in adenine

One of these two-state conical intersection seams is explored here. Starting from the three-state conical intersection *ci*123 (Figure 6a) or *ci*123′ (Figure 6b) the S_1-S_2 two-state conical intersection minimum was optimized. Because the initial point was already on the seam, the search moved along the seam until it found the minimum-energy point, *ci*12. The resulting paths are energy-minimized sections of the seam connecting each of the three-state conical intersections, with the minimum-energy point of the two-state conical intersection *ci*12. Figure 6 shows the energies of the ground and four excited states as a function of the bond distance $R(C^2-N^3)$. Although all coordinates change during the optimization (there are no geometrical constraints imposed), the bond distance $R(C^2-N^3)$ is chosen to be plotted because it changes smoothly along both paths. It increases from 1.33 to 1.39 Å along the path from *ci*123 to *ci*12 and decreases from 1.45 to 1.39 Å along the path from *ci*123′ to *ci*12. The energy of the resulting two-state conical intersection is 5.5 eV at the MRCI1 level and 5.3 eV at the MRCI$\sigma\pi$ (see Table 2) and is lower than all excitation energies. An S_1-S_2 conical intersection involving $\pi\pi^*$ and $n\pi^*$ states has been reported recently by Perun et al.[44] Figure 7 shows the two vectors spanning the branching plane for *ci*12 at the minimum-energy point of the seam. The coupling mode a'' corresponds to the coupling between the $\pi\pi^*$ and $n\pi^*$ states and resembles out-of-plane coupling modes of the *ci*123 and *ci*123′ three-state conical intersections. This is expected because *ci*123 and *ci*123′ include this pair of states, and its coupling should be part of their five branching vectors. This a'' mode involves mainly motion of the $N^1-C^2-N^3$ moiety. The a' mode involves in-plane distortions of the six-membered ring.

3.3. Effect of Electron Correlation on the Location of Conical Intersections. When locating conical intersections in systems of the size of uracil and adenine, one is forced to use a method that does not include all the required correlation and is less accurate than the method used to calculate energies at single points on the potential energy surface. For this reason, the energy differences obtained at the lower level of theory (here MRCI1) are different from the ones at the higher level (MRCI$\sigma\pi$), and the predicted points of conical intersections are shifted. Furthermore, different points on the surface and different states gain different correlation energy. For example, the energy of the S_1 state in adenine is not affected by dynamical correlation at $\boldsymbol{R}_e(S_0)$ but is lowered by 0.46 eV at the distorted geometry $\boldsymbol{R}_x$(*ci*123′). How close the conical intersection predicted at the lower level of theory is to the one at a higher level of theory depends on the particular case and varies between different crossings, even within the same molecule. In this study, the *ci*123 conical intersection in adenine is located more accurately than that of the *ci*123′ at the MRCI1 level. The separation of energies at the MRCI$\sigma\pi$ level is an indication of the quality of prediction of the conical intersection at the MRCI1 level. The *ci*012 conical intersection in uracil is also poorly described at MRCI1. These energies are given in Tables 1 and 2 and are discussed in detail in the previous sections.

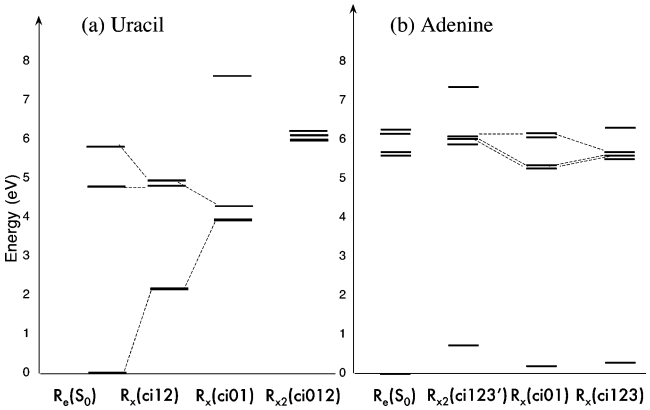

Figure 8. Diagram of the energy levels at the main points discussed in this work using MRCI$\sigma\pi$; (a) the S_0, S_1, S_2 states of uracil and (b) S_0, S_1, S_2, S_3, S_4 states of adenine.

In this work, a procedure was used in which an intermediate expansion was used to refine the conical intersection if the energy difference of the states that should be degenerate at the MRCI$\sigma\pi$ level was more than 0.3 eV. Optimization could not be done at the MRCI$\sigma\pi$ level because the size of this expansion was more than 100 million CSFs. So, whenever the small expansion was inadequate, an intermediate expansion was used to locate the conical intersections. The choice of the particular intermediate expansion MRCIσ was based on the fact that single excitations from the σ orbitals were found to be important for more accurately calculating the excitation energies in uracil.[42] Qualitatively, the conical intersection does not change much between the different expansions in general. In uracil, the reoptimization of the three-state conical intersection changed the energy difference between the states from 0.6 to 0.2 eV. The average of the three energies changed from 6.19 to 6.16 eV. The bond lengths changed from 0.01 to 0.06 Å, and the angles changed from 0 to 18°. The 18° occurred in one dihedral angle, while most of the other angles had very small changes. The energy difference in adenine changed from 0.4 to 0.2 eV. The average of the energies of the three states changed from 5.93 to 5.99 eV. The average bond distance change was 0.02 Å, with the largest being 0.07 Å, and the largest angle change was 3°.

4. Conclusions

In this work, the existence of three-state conical intersections in the nucleobases uracil and adenine has been investigated. Figure 8 summarizes the energetics of the points of interest for both molecules and aims at emphasizing their differences. A

three-state conical intersection between the S_0, S_1, and S_2 states has been located in uracil at an energy 6.2 eV above the ground-state minimum energy. This energy is ca. 0.4 eV higher than vertical excitation to S_2, 1.3 eV higher than the S_1-S_2 two-state conical intersection, and 2 eV higher than the S_1-S_0 conical intersection found previously. Consequently, this crossing is less likely to be directly involved in a radiationless decay mechanism. Figure 8a shows the energies of all conical intersections, and dotted lines connect the points between which pathways have been found previously.[42] The connected points represent the radiationless decay mechanism, and clearly, there is no access to the three-state conical intersection.

In adenine, two different three-state degeneracies between the S_1, S_2, and S_3 states have been located at energies close to the vertical excitation energies. These three-state conical intersections are at energies 5.6 and 6.0 eV above the ground-state minimum, respectively. Vertical excitation energies to the two bright states are at 5.7 and 6.1 eV, so the crossings are at similar energies and will probably participate in radiationless pathways that quench fluorescence in adenine. The energies of these points and how they can be connected are shown in Figure 8b. The existence of two different seams of three-state conical intersections indicates that these features are common and complicate the potential energy surfaces of adenine. Furthermore, the presence of three-state conical intersections implies that seams of two-state conical intersections between pairs of these states are branching out of the three-state seam, and these two-state seams are at energies lower than the three-state one. We have calculated points of one of these seams, an S_1-S_2 seam, that connects the two different three-state conical intersections found here.

It has been stated frequently in the past that the dynamics and spectra of excited states in adenine and the other purine bases are affected by the interactions of two excited states. In this work, it is shown that the picture can be a lot more complicated with three or four excited states interacting and crossing. Here, the focus has been on the location of three-state conical intersections. Although the results indicate the potential involvement of three-state conical intersections, further work is needed to verify this involvement. Pathways connecting all the features and any barriers along these pathways are needed. Ultimately, nuclear dynamics can determine the effect of these features in the spectroscopy and dynamics of excited states in adenine.

The above results suggest a high frequency of three-state conical intersections in adenine and probably other systems with similar high density of excited states. We anticipate the presence of three-state conical intersections in the other nucleobases. More generally conjugated systems with many excited states and many degrees of freedom are likely to exhibit three-state conical intersections, as well.

Acknowledgment. This work was supported by the National Science Foundation under Grant No. CHE-0449853 and Temple University.

Supporting Information Available: Tables of internal coordinates for uracil and adenine are given that correspond to geometries optimized and described in the text. This material is available free of charge via the Internet at http://pubs.acs.org.

References and Notes

(1) Klessinger, M.; Michl, J. *Excited States and Photochemistry of Organic Molecules*; VCH Publishers: New York, 1995.
(2) Domcke, W.; Yarkony, D. R.; Köppel, H. *Conical Intersections*; World Scientific: Singapore, 2004.
(3) Bersuker, I. B. *The Jahn−Teller Effect and Vibronic Interactions in Modern Chemistry*; Plenum Press: New York, 1984.
(4) Katriel, J.; Davidson, E. R. *Chem. Phys. Lett.* **1980**, *76*, 259−262.
(5) Robb, M. A.; Garavelli, M.; Olivucci, M.; Bernardi, F. *Rev. Comput. Chem.* **2000**, *15*, 87.
(6) Yarkony, D. R. *J. Phys. Chem. A* **2001**, *105*, 6277−6293.
(7) Keating, S. P.; Mead, C. A. *J. Chem. Phys.* **1985**, *82*, 5102−5117.
(8) Han, S.; Yarkony, D. R. *J. Chem. Phys.* **2003**, *119*, 11562−11569.
(9) Han, S.; Yarkony, D. R. *J. Chem. Phys.* **2003**, *119*, 5058−5068.
(10) Coe, J. D.; Martinez, T. J. *J. Am. Chem. Soc.* **2005**, *127*, 000.
(11) von Neumann, J.; Wigner, E. P. *Phys. Z.* **1929**, *30*, 467.
(12) Matsika, S.; Yarkony, D. R. *J. Chem. Phys.* **2002**, *117*, 6907.
(13) Matsika, S.; Yarkony, D. R. *J. Am. Chem. Soc.* **2003**, *125*, 10672−10676.
(14) Matsika, S.; Yarkony, D. R. *J. Am. Chem. Soc.* **2003**, *125*, 12428−12429.
(15) Blancafort, L.; Robb, M. A. *J. Phys. Chem. A* **2004**, *108*, 10609−10614.
(16) Kato, S.; Hoenigman, R.; Gianola, A.; Ichino, T.; Bierbaum, V.; Lineberger, W. C. In *Molecular Dynamics and Theoretical Chemistry Contractors Review*; Berman, M., Ed.; AFOSR, Shelter Point Hotel: San Diego, 2003; pe 49.
(17) Crespo-Hernandez, C. E.; Cohen, B.; Hare, P. M.; Kohler, B. *Chem. Rev.* **2004**, *104*, 1977.
(18) Daniels, M.; Hauswirth, W. *Science* **1971**, *171*, 675.
(19) Daniels, M. In *Photochemistry and Photobiology of Nucleic Acids*; Wang, S. Y., Ed.; Academic Press: New York, 1976; Vol. 1 p 23.
(20) Callis, P. R. *Annu. Rev. Phys. Chem.* **1983**, *34*, 329.
(21) Pecourt, J.-M. L.; Peon, J.; Kohler, B. *J. Am. Chem. Soc.* **2000**, *122*, 9348−9349.
(22) Pecourt, J.-M. L.; Peon, J.; Kohler, B. *J. Am. Chem. Soc.* **2001**, *123*, 10370−10378.
(23) Cohen, B.; Hare, P.; Kohler, B. *J. Am. Chem. Soc.* **2003**, *125*, 13594−13601.
(24) Cohen, B.; Crespo-Hernandez, C. E.; Kohler, B. *Faraday Discuss.* **2004**, *127*, 000.
(25) Peon, J.; Zewail, A. H. *Chem. Phys. Lett.* **2001**, *348*, 255−262.
(26) Gustavsson, T.; Sharonov, A.; Markovitsi, D. *Chem. Phys. Lett.* **2002**, *351*, 195−200.
(27) Gustavsson, T.; Sharonov, A.; Onidas, D.; Markovitsi, D. *Chem. Phys. Lett.* **2002**, *356*, 49.
(28) Onidas, D.; Markovitsi, D.; Marguet, S.; Sharonov, A.; Gustavsson, T. *J. Phys. Chem. B* **2002**, *106*, 11367.
(29) Brady, B. B.; Peteanu, L.; Levy, D. H. *Chem. Phys. Lett.* **1988**, *147*, 538−543.
(30) Nir, E.; Kleinermanns, K.; Grace, L.; de Vries, M. S. *J. Phys. Chem. A* **2001**, *105*, 5106−5110.
(31) Piuzzi, F.; Mons, M.; Dimicoli, I.; Tardivel, B.; Zhao, Q. *Chem. Phys.* **2001**, *270*, 205−214.
(32) Lührs, D. C.; Viallon, J.; Fischer, I. *Phys. Chem. Chem. Phys.* **2001**, *3*, 1827.
(33) He, Y.; Wu, C.; Kong, W. *J. Phys. Chem. A* **2003**, *107*, 5145−5148.
(34) He, Y.; Wu, C.; Kong, W. *J. Phys. Chem. A* **2004**, *108*, 943−949.
(35) Kang, H.; Lee, K. T.; Jung, B.; Ko, Y. J.; Kim, S. K. *J. Am. Chem. Soc.* **2002**, *124*, 12958.
(36) Kang, H.; Jung, B.; Kim, S. K. *J. Chem. Phys.* **2003**, *118*, 6717.
(37) Kim, N. J.; Jeong, G.; Kim, Y. S.; Sung, J.; Kim, S. K.; Park, Y. D. *J. Chem. Phys.* **2000**, *113*, 10051.
(38) Ullrich, S.; Schultz, T.; Zgierski, M. Z.; Stolow, A. *J. Am. Chem. Soc.* **2004**, *126*, 2262.
(39) Ullrich, S.; Schultz, T.; Zgierski, M. Z.; Stolow, A. *Phys. Chem. Chem. Phys.* **2004**, *6*, 2796−2801.
(40) Ismail, N.; Blancafort, L.; Olivucci, M.; Kohler, B.; Robb, M. A. *J. Am. Chem. Soc.* **2002**, *124*, 6818−6819.
(41) Merchán, M.; Serrano-Andrés, L. *J. Am. Chem. Soc.* **2003**, *125*, 8108−8109.
(42) Matsika, S. *J. Phys. Chem. A* **2004**, *108*, 7584−7590.
(43) Sobolewski, A. L.; Domcke, W. *Eur. Phys. J. D* **2002**, *20*, 369−374.
(44) Perun, S.; Sobolewski, A. L.; Domcke, W. *J. Am. Chem. Soc.* **2005**, *127*, 6257−6265.
(45) Dunning, T. H. *J. Chem. Phys.* **1970**, *53*, 2823.
(46) Lischka, H.; Shepard, R.; Pitzer, R. M.; Shavitt, I.; Dallos, M.; Myller, T.; Szalay, P. G.; Seth, M.; Kedziora, G. S.; Yabushita, S.; Zhang, Z. *Phys. Chem. Chem. Phys.* **2001**, *3*, 664.
(47) Lischka, H.; Dallos, M.; Szalay, P. G.; Yarkony, D. R.; Shepard, R. *J. Chem. Phys.* **2004**, *120*, 7322.
(48) Dallos, M.; Lischka, H.; Shepard, R.; Yarkony, D. R.; Szalay, P. G. *J. Chem. Phys.* **2004**, *120*, 7330.
(49) Lischka, H.; Dallos, M.; Shepard, R. *Mol. Phys.* **2002**, *100*, 1647.

(50) Broo, A.; Holmén. *Chem. Phys.* **1996**, *211*, 147.
(51) Broo, A. *J. Phys. Chem. A* **1998**, *102*, 526.
(52) Mennucci, B.; Toniolo, A.; Tomasi, J. *J. Phys. Chem. A* **2001**, *105*, 4749−4757.
(53) Jean, J. M.; Hall, K. B. *J. Phys. Chem. A* **2000**, *104*, 1937.
(54) Salter, L. M.; Chaban, G. M. *J. Phys. Chem. A* **2002**, *106*, 4251.
(55) Mishra, S. K.; Shukla, M. K.; Mishra, P. C. *Spectrochim. Acta, Part A* **2000**, *56*, 1355.
(56) Fülscher, M. P.; Serrano-Andres, L.; Roos, B. O. *J. Am. Chem. Soc.* **1997**, *119*, 6167−6176.
(57) Clark, L. B.; Peschel, G. G.; Tinoco, I., Jr. *J. Phys. Chem.* **1965**, *69*, 3615.
(58) Atchity, G. J.; Xantheas, S. S.; Ruedenberg, K. *J. Chem. Phys.* **1991**, *95*, 1862.
(59) Schaftenaar, G.; Noordik, J. *J. Comput.-Aided Mol. Design* **2000**, *14*, 123−134.